OXFORD

Human Molecular Genetics, 2017, Vol. 26, No. 4 781–789

doi: 10.1093/hmg/ddw430
Advance Access Publication Date: 30 December 2016
Original Article

ORIGINAL ARTICLE

A conserved retromer sorting motif is essential for mitochondrial DLP1 recycling by VPS35 in Parkinson's disease model

Wenzhang Wang[1], Xiaopin Ma[1], Leping Zhou[1,2], Jun Liu[2,*] and Xiongwei Zhu[1,*]

[1]Department of Pathology, Case Western Reserve University, Cleveland, OH 44106, USA and [2]Department of Neurology and Institute of Neurology, Ruijin Hospital, Shanghai Jiao Tong University School of Medicine, Shanghai 200020, People's Republic of China

*To whom correspondence should be addressed at: X.Z.: Tel.: 001-216-3685903; Email: xiongwei.zhu@case.edu and J.L.: Tel.: 086-21-64454473; Email: jly0520@hotmail.com.

Abstract

Impaired mitochondria dynamics and quality control are involved in mitochondrial dysfunction and pathogenesis of Parkinson's disease (PD). VPS35 mutations cause autosomal dominant PD and we recently demonstrated that fPD-associated VPS35 mutants can cause mitochondrial fragmentation through enhanced VPS35-DLP1 interaction. In this study, we focused on the specific sites on DLP1 responsible for the VPS35-DLP1 interaction. A highly conserved FLV motif was identified in the C-terminus of DLP1, mutation of which significantly reduced VPS35-DLP1 interaction. A decoy peptide design based on this FLV motif could block the VPS35-DLP1 interaction and inhibit the recycling of mitochondrial DLP1 complexes. Importantly, VPS35 D620N mutant-induced mitochondrial fragmentation and respiratory deficits could be rescued by the treatment of this decoy peptide in both M17 cells overexpressing D620N or PD fibroblasts bearing this mutation. Overall, our results lend further support to the notion that VPS35-DLP1 interaction is key to the retromer-dependent recycling of mitochondrial DLP1 complex during mitochondrial fission and provide a novel therapeutic target to control excessive fission and associated mitochondrial deficits.

Introduction

Parkinson's disease (PD) is the second most common neurodegenerative disease after Alzheimer disease and affects 1% of the aged population worldwide. Individuals with PD display variable motor symptoms including resting tremor, bradykinesia, rigidity and postural instability (1). Some PD patients also present variable non-motor symptoms such as cognitive impairment, mood disorders, and speech and swallowing problems (2). The major pathological hallmarks of PD consist of accumulation of α-synuclein and ubiquitin in Lewy bodies in affected neurons and selective loss of dopaminergic neurons in the midbrain (3,4). Although the majority of PD cases are sporadic, decades of genetic studies of PD pedigrees have revealed dozens of genes involved in the development of familial PD including α-synuclein and LRRK2 associated with autosomal dominant fPD, and PINK1, Parkin, DJ-1 associated with autosomal recessive fPD (5). Research on these genetic factors proved crucial in the current understanding of pathogenic mechanisms of PD.

Studies on neurotoxin models and multiple genetic factors of PD revealed that mitochondrial dysfunction likely represents a critical step during the pathogenesis of PD (6,7). MPTP, a specific inhibitor of complex I of the electron transport chain, causes selective dopaminergic neuronal loss and associated motor dysfunction in rodents and primates and Parkinsonism

Received: November 7, 2016. **Revised:** November 7, 2016. **Accepted:** December 16, 2016

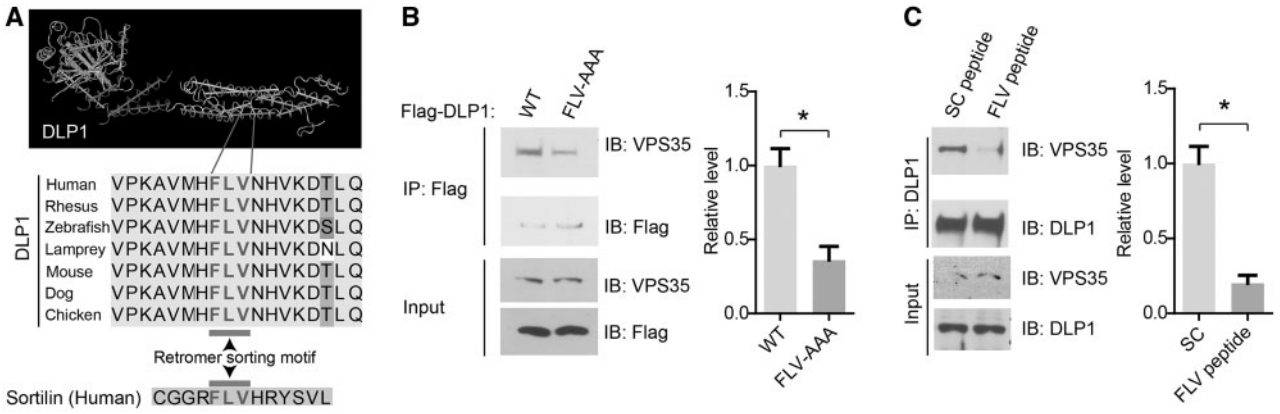

Figure 1. A conserved VPS35 recognition motif in DLP1. (**A**) 3D protein structure of DLP1 was retrieved from Protein Structure Database (NCBI) and was visualized by Cn3D software (top). A conserved retromer sorting motif (FLV) is located at C-terminal of DLP1 protein (bottom). (**B**) Representative western blot analysis (left) and quantification (right) of VPS35 in Flag immunoprecipitates from cell lysates prepared from M17 cells transfected with flag-tagged wild-type (WT) DLP1 or triple alanine mutant DLP1 at the FLV motif (FLV-AAA). (**C**) Representative western blot analysis (left) and quantification (right) of VPS35 in DLP1 immunoprecipitates from cell lysates prepared from M17 cells subject to 24 h treatment of FLV peptide or scramble peptide (SC peptide). Data are means ± s.e.m of three independent experiments. Statistics: one-way analysis of variance (ANOVA) followed by Tukey's multiple comparison test. $^*P < 0.05$.

in humans (4). Our recent study demonstrated that DLP1-dependent mitochondrial fragmentation plays an essential role in mediating MPP^+-induced mitochondrial and neuronal toxicity (8). Many of the PD genetic factors such as α-synuclein, PINK1, Parkin, LRRK2, and DJ-1 are localized to mitochondria and induce defective mitochondrial respiration (7). More recently, expanding evidence suggests that these genetic factors are involved in the regulation of mitochondrial dynamics and PD-causing mutations cause alterations in mitochondrial morphology, abnormal intracellular trafficking and impaired mitochondrial quality control (9–14), suggesting that abnormal mitochondrial dynamics may be a common pathway in mediating mitochondrial dysfunction during the pathogenesis of PD.

Recently, it was found that the PD genetic locus (PARK17) encodes the genetic variant in vacuolar protein sorting-associated protein 35 (VPS35) which results in autosomal-dominant late-onset familial PD (15,16). VPS35 mutations were also found in sporadic PD (15,16). VPS35 is the largest subunit of heteropentameric mammalian retromer. Retromer is a 'master conductor' of endosomal sorting and trafficking (17) which plays an essential role in the endosome-to-Golgi and endosome-to-plasma membrane retrieval of membrane proteins (18,19). Retromer is also involved in transporting cargo from the mitochondria to the peroxisomes (20). Retromer consists of two subcomplexes: a cargo recognition complex composed of VPS35, VPS29 and VPS26, and a SNX-BAR dimer including combinations of SNX1, 2, 5, or 6 (21). VPS35 functions as the central subunit to which VPS29 and VPS26 bind independently and it binds to sorting motifs present in the cytoplasmic domains of cargo proteins during the retrieval process (22). The pathogenic mechanism underlying PD-causing VPS35 mutation is under intensive investigation. It has been suggested that the VPS35 PD mutants had little effect on the assembly of VPS35-VPS26-VSP29 complex but rather perturbed cargo recognition and binding of retromer complex (23–26). Recent studies from two groups including ours found that mutant VPS35 caused extensive mitochondrial fragmentation and mitochondrial dysfunction both *in vitro* and *in vivo* (26,27), supporting the notion that abnormal mitochondrial dynamics is causally involved in mitochondrial dysfunction critical to the pathogenesis of PD. Tang et al. suggested that VPS35 mutant causes mitochondrial fragmentation likely through Mul-1 accumulation (27) which was known to degrade fusion factor Mfn2 (28), although how VPS35 regulates Mul-1 expression remains elusive. We found that PD-associated VPS35 mutant caused excessive fission through an increased VPS35-DLP1 interaction which enhanced the retromer-dependent turnover of fission-inhibitory mitochondrial DLP1 complexes via the mitochondrial derived vesicle-dependent trafficking and lysosomal degradation (26). In this study, we further identified a conserved cargo recognition motif on DLP1 and demonstrated that a decoy peptide design based on such motif interrupted VPS35-DLP1 interaction and rescued VPS35 mutation-induced mitochondrial fragmentation and mitochondrial dysfunction, thus providing further evidence to support our model.

Results

A conserved VPS35 recognition motif in DLP1 is essential for VPS35-DLP1 interaction

We recently reported that retromer mediates the transport of mitochondrial DLP1 complexes to lysosomes for recycling through direct interaction between VPS35 and DLP1 (26). Proteins that traffic in the endomembrane system often contain sorting motifs that function to direct the transport of protein between the various compartments (29). To determine the retromer binding site in DLP1, the sequence of DLP1 protein from various species was compared (Fig. 1A) to identify highly conserved regions which may contain retromer sorting motif. Indeed, a highly conserved FLV motif in the C-terminal of DLP1 protein that resembles the retromer sorting motif found in the Sortilin (29), a well characterized retromer cargo, was identified (Fig. 1A). To determine whether this FLV motif in DLP1 is causally involved in the VPS35-DLP1 interaction, we performed alanine mutagenesis analysis by mutating FLV into triple alanine and transfected M17 human dopaminergic neuroblastoma cells with plasmids expressing either flag-DLP1 or flag-DLP1 with FLV motif mutation (FLV-AAA). Co-immunoprecipitation analysis revealed that mutant DLP1 (FLV-AAA) showed significantly decreased binding ability to VPS35 in M17 cells compared with WT DLP1 (Fig. 1B). Furthermore, based on the sequence of FLV sorting motif in DLP1, a decoy peptide that contains FLV and its flanking sequence (FLV peptide) was designed and synthesized

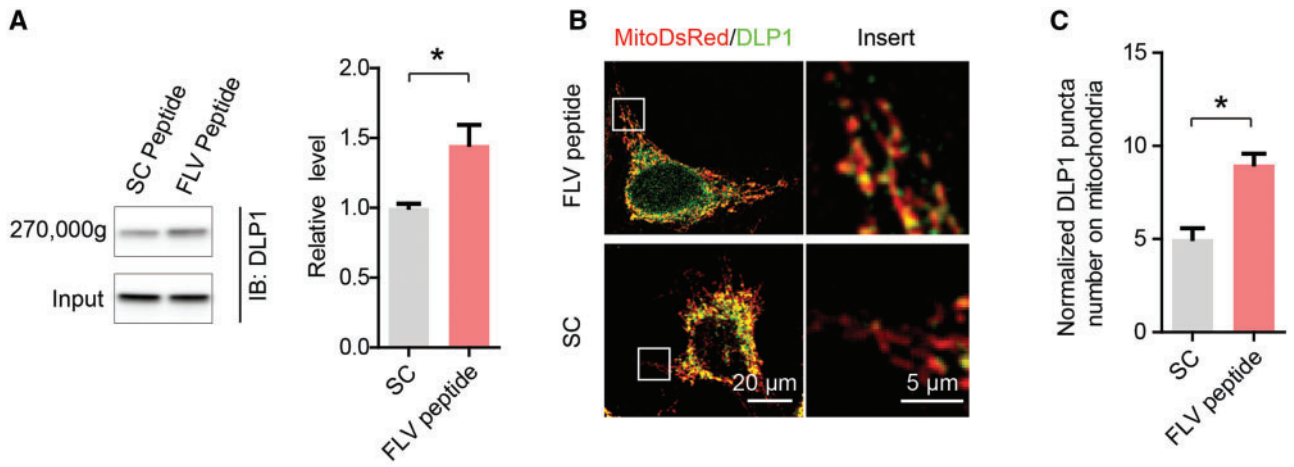

Figure 2. FLV peptide inhibited the recycling of mitochondrial DLP1 complexes. (**A**) DLP1 levels in the ultracentrifugation (270,000 g) precipitates of mitochondrial fraction from FLV peptide- or scramble peptide-treated M17 cells exposed to DTME. M17 cells were treated with 0.5 mM reversible and membrane permeable crosslinker dithiobismaleimidoethane (DTME) for 5 min. After cell lysis, mitochondrial fractions were prepared and further subjected to ultracentrifugation (270,000 g) to sediment large protein complexes. The ultracentrifugation precipitates and input were analysed by SDS-PAGE and western blot for DLP1 detection (left) and quantification (right). (**B**) Immunostaining of DLP1 in FLV peptide- or scramble peptide-treated M17 cells transfected with mito-DsRed2. Representative confocal images (left) and enlargement (right) of the boxed area showing the localization of DLP1 puncta (green) on mitochondria (red). (**C**) Quantification of the number of DLP1 puncta on mitochondria in M17 cells treated with FLV peptide or scramble peptide. Data are means ± s.e.m of three independent experiments. Statistics: one-way analysis of variance (ANOVA) followed by Tukey's multiple comparison test. *$P < 0.05$.

to compete with the binding of DLP1 to VPS35. Indeed, co-immunoprecipitation analysis revealed that VPS35-DLP1 interaction is significantly reduced in the M17 cells treated with FLV peptide compared with that of scramble peptide-treated M17 cells (Fig. 1C). Collectively, these data suggest that FLV motif in DLP1 is essential for its interaction with VPS35.

FLV peptide inhibited the recycling of mitochondrial DLP1 complexes in M17 cells

We previously demonstrated that D620 of VPS35 is essential in the interaction between VPS35 and DLP1 which is key to the recycling of mitochondrial DLP1 complexes (26). Since FLV motif of DLP1 is essential for the VPS35-DLP1 interaction, we then investigated whether FLV peptide impacts the recycling of mitochondrial DLP1 complexes. To determine the levels of mitochondrial DLP1 complexes, large mitochondrial protein complexes were precipitated by ultracentrifugation (270,000 g) of mitochondrial fractions prepared from FLV peptide- or scramble peptide-treated M17 cells exposed to the reversible crosslinking agent (i.e., DTME) and analysed by SDS-PAGE. DLP1 levels were significantly increased in these ultracentrifugation precipitates from the M17 cells treated with FLV peptide as compared to that of scramble peptide-treated cells (Fig. 2A). To corroborate this finding, we further imaged mitochondrial DLP1 in fixed M17 cells after DLP1 immunostaining (Fig. 2B). Consistently, the density of the mitochondrial DLP1 puncta, representing large mitochondrial DLP1 complexes (30), was significantly increased in M17 cells treated with FLV peptide as compared to that of scramble peptide-treated M17 cells (Fig. 2C).

FLV peptide rescued mitochondrial fragmentation in M17 cells overexpressing VPS35

VPS35-DLP1 interaction is essential for efficient mitochondrial fission and PD pathogenic VPS35 mutation caused mitochondrial fragmentation and dysfunction through its enhanced interaction with DLP1 (26). Since FLV motif in DLP1 was required for VPS35-DLP1 interaction, we hypothesized that FLV peptide, by inhibiting the VPS35-DLP1 interaction, could tip the balance of mitochondrial fission/fusion and alleviate abnormal mitochondrial morphology and dysfunction in cells expressing PD pathogenic VPS35 mutations. To visualize mitochondria, M17 cells were transiently transfected with mito-DsRed2, a red fluorescent protein that specifically targets the mitochondrial matrix. Two days after transfection, cells were treated with either scramble peptide or FLV peptide for 24 h and fixed, stained and imaged by laser confocal microscopy. In M17 cells treated with scramble peptide, mitochondria demonstrate a tubular and filamentous morphology, similar to the untreated M17 cells. However, in M17 cells treated with the FLV peptide, mitochondria became elongated and connected with the aspect ratio (a ratio between the major and the minor axes of the ellipse equivalent to the mitochondria as an index for mitochondrial morphology) being significantly increased compared with that of scramble peptide-treated M17 cells (Fig. 3A and B). More importantly, the appearance of small round structures representing fragmented mitochondria in M17 cells stably overexpressing WT or mutant VPS35 (D620N and R524W) was unchanged by the treatment of scramble peptide, but was replaced by the appearance of much longer mitochondrial tubules in these cells by the treatment of FLV peptide (Fig. 3A). Quantification analysis revealed that FLV treatment restored the aspect ratio in these cells to a level comparable to that of vector control M17 cells (Fig. 3B). To exclude the potential off-target effect of FLV peptide, we measured general retromer sorting activity of cells by studying the recycling of CD36, a recognized VPS35 substrate, and found that neither scrambled peptide nor FLV peptide had any effect on CD36 recycling in vector control or VPS35 overexpressing M17 cells (Supplementary Material, Fig. S1).

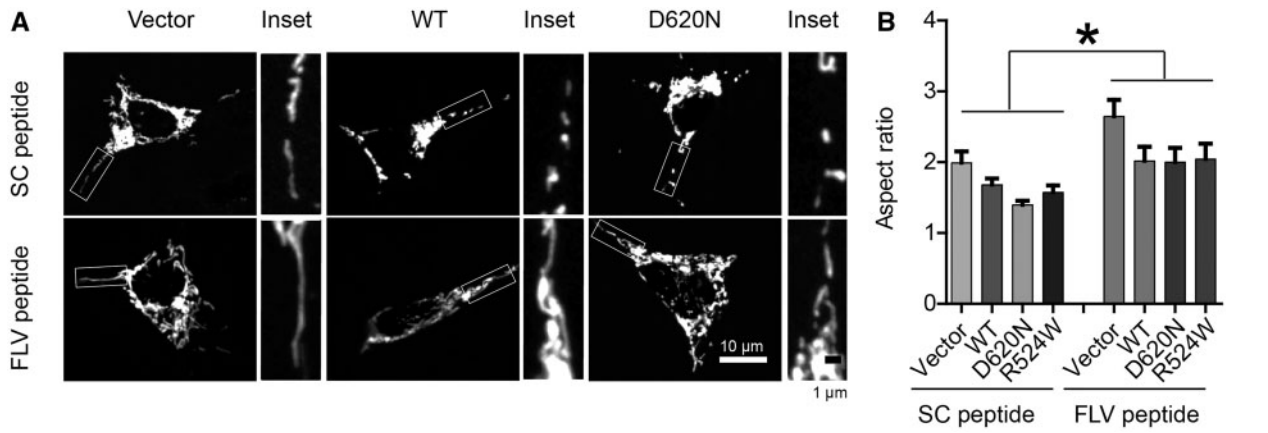

Figure 3. FLV peptide rescued mitochondrial fragmentation in M17 cells overexpressing VPS35. (**A**) Representative pictures of mitochondria, visualized by mito-DsRed2 fluorescence signal, in M17 cells overexpressing WT VPS35 or fPD-associated VPS35 mutants treated with scrambled peptide or FLV peptide. The boxed area was enlarged to the right of each picture. (**B**) Quantification of mitochondrial aspect ratio in M17 cell overexpressing WT VPS35 or fPD-associated VPS35 mutants treated with scramble peptide or FLV peptide. Data are means ± s.e.m of 3 independent experiments. Statistics: one-way analysis of variance (ANOVA) followed by Tukey's multiple comparison test. *$P < 0.05$.

FLV peptide rescued mitochondrial dysfunction caused by VPS35 D620N mutation in M17 cells

We next investigated the effects of FLV peptide on mitochondrial function by measuring OXPHOS respiration activity of M17 cells stably overexpressing VPS35 D620N mutant or vector control M17 cells exposed to FLV peptide or scramble peptide using Seahorse XF24 extracellular flux analyzer. No difference was noted in the Vector control M17 cells between the treatment of FLV peptide or scramble peptide (Fig. 4A). However, in M17 cells stably overexpressing VPS35 D620N mutant, the significantly decreased basal and maximal oxygen consumption rate (OCR) were almost completely rescued by the treatment with FLV peptide but not by the scramble peptide. Further analysis revealed that the impaired respiratory control ratio (Fig. 4B) and decreased spare respiratory capacity (Fig. 4C) in VPS35 D620N M17 cells were also rescued by FLV peptide treatment to a level that was comparable to the Vector control M17 cells, but not by scramble peptide treatment.

FLV peptide rescued mitochondria defects in human fibroblasts from PD patient bearing VPS35 D620N mutation

We further investigated the rescuing effects of FLV peptide on mitochondrial fragmentation and respiratory dysfunction in human fibroblasts from a PD patient bearing the VPS35 D620N mutation. In normal healthy fibroblasts (NHFs), no significant changes caused by FLV peptide or scramble peptide treatment in the mitochondrial morphology were noted (Fig. 5A and B). However, significant changes in mitochondrial morphology were found by the treatment of FLV peptide, but not by the scramble peptide, in PD D620N fibroblasts: the significantly fragmented mitochondria observed in untreated (not shown) or scramble peptide-treated PD fibroblasts became more elongated and connected after FLV peptide treatment (Fig. 5A). Quantification analysis confirmed that FLV peptide led to a significant increase in mitochondrial length in PD D620N fibroblasts compared to that of untreated or scramble peptide treated PD D620N fibroblasts (Fig. 5B).

Accompanying the restoration of mitochondrial morphology after FLV peptide treatment in PD D620N fibroblasts, the impaired basal and maximal respiration in VPS35 D620N fibroblasts were also rescued after the treatment of FLV peptide, but not scramble peptide, to a level that is more comparable to that of NHF fibroblasts (Fig. 6). More detailed analysis confirmed that FLV peptide restored the respiratory control ratio and spare respiration capacity in the VPS35 D620N fibroblasts (Fig. 6).

Discussion

The major finding of this study is that we identified a conserved FLV motif in the C-terminus of DLP1 responsible for the recognition and binding of DLP1 by VPS35. In this study, we first identified an FLV motif that is highly conserved from zebrafish to human which resembles the retromer sorting motif in the well-characterized retromer cargo, Sortilin. Then, by using both genetic mutagenesis and a carefully designed decoy peptide (i.e., FLV peptide) to interrupt VPS35-DLP1 interaction, we demonstrated that this FLV motif in DLP1 is critical for the VPS35-DLP1 interaction. We further demonstrated by both confocal microscopy and biochemical assay that FLV peptide treatment led to increased mitochondrial DLP1 puncta density and increased DLP1 levels in the ultracentrifuge precipitates of the mitochondrial fraction reflecting accumulation of mitochondrial DLP1 complexes. Importantly, FLV peptide treatment alleviated VPS35 D620N-induced mitochondrial fragmentation and respiratory deficits both in M17 neurons overexpressing VPS35 D620N and in fibroblasts from PD patient bearing the D620N mutation.

This study was built upon our recent finding of interaction between VPS35 and DLP1(26). In this prior study, we demonstrated that the D620 site of VPS35 plays a critical role in the VPS35-DLP1 interaction. In the current study, we focused on the identification of specific sites on DLP1 responsible for the VPS35-DLP1 interaction. VPS35 binds to cargos through a conserved sorting motif in target proteins (29,31,32), which is important for VPS35's recognition of cargos. Indeed, we found a conserved retromer sorting motif, FLV, in the C-terminal of DLP1 protein. When we mutated the FLV motif to AAA, the interaction between DLP1 and VPS35 was significantly impaired

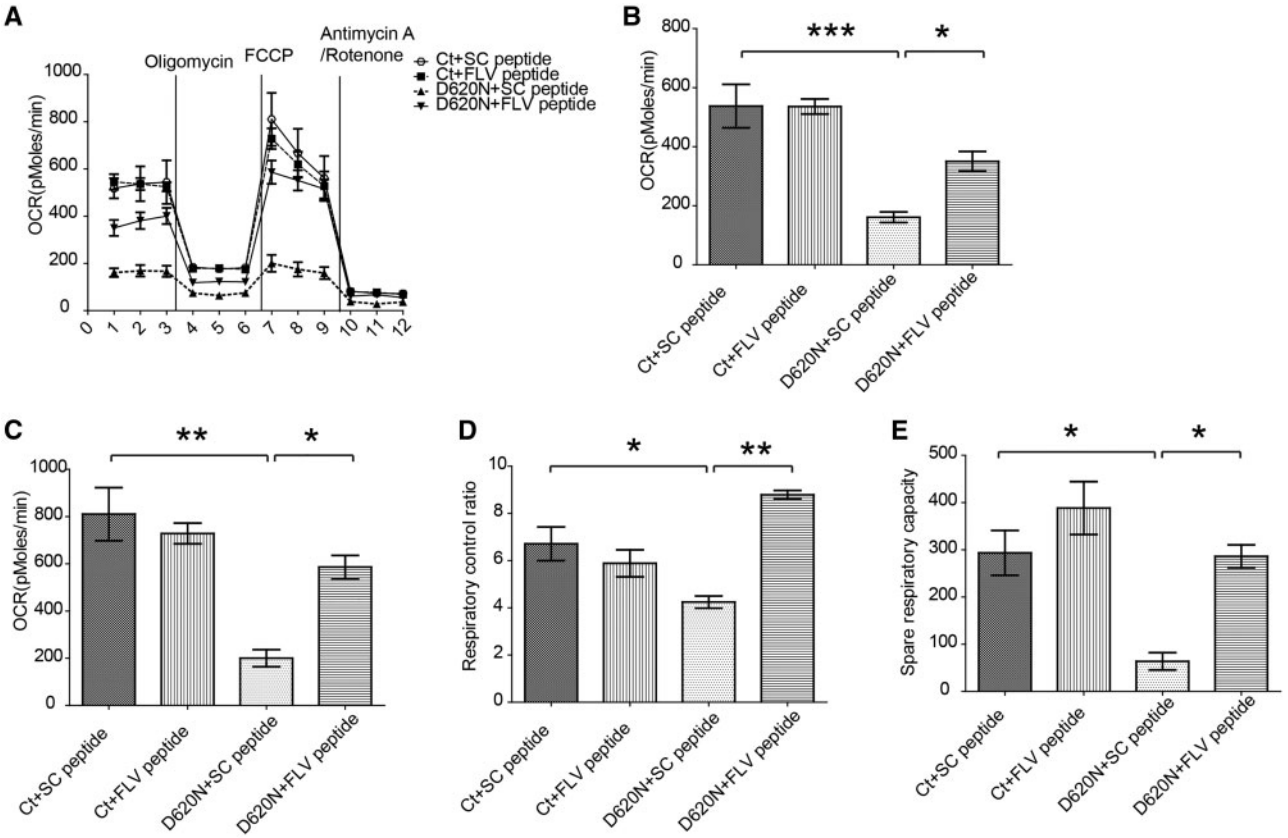

Figure 4. FLV peptide rescued mitochondrial respiration deficits in M17 cells overexpressing D620N VPS35 mutant. (**A**) Mitochondria respiration activity was measured by Seahorse assay in M17 cells overexpressing vector (Ct) or VPS35 D620N mutant treated with scramble peptide or FLV peptide. Oxygen consumption (OCR) rate was measured before and after cells being sequentially exposed to oligomycin (inhibits ATP synthase, blocks oxygen consumption related to ATP synthesis), FCCP (uncoupler to assess maximal OCR), and antimycin A/rotenone (blocks electron flux through both complex I and II). (**B–E**) Quantification in these M17 cells of Basal OCR (B), Maximal OCR (C, OCR_{FCCP}), Respiratory control ratio (D, $OCR_{FCCP}/OCR_{Oligomycin}$), and Spare respiratory capacity (OCR_{FCCP}-OCR_{Basal}) were calculated after subtracting the non-mitochondrial respiration (E, $OCR_{Antimycin\ A/rotenone}$). Data are means ± s.e.m of 3 independent experiments. Statistics: one-way analysis of variance (ANOVA) followed by Tukey's multiple comparison test. $^{*}P < 0.05$, $^{**}P < 0.01$ and $^{***}P < 0.001$.

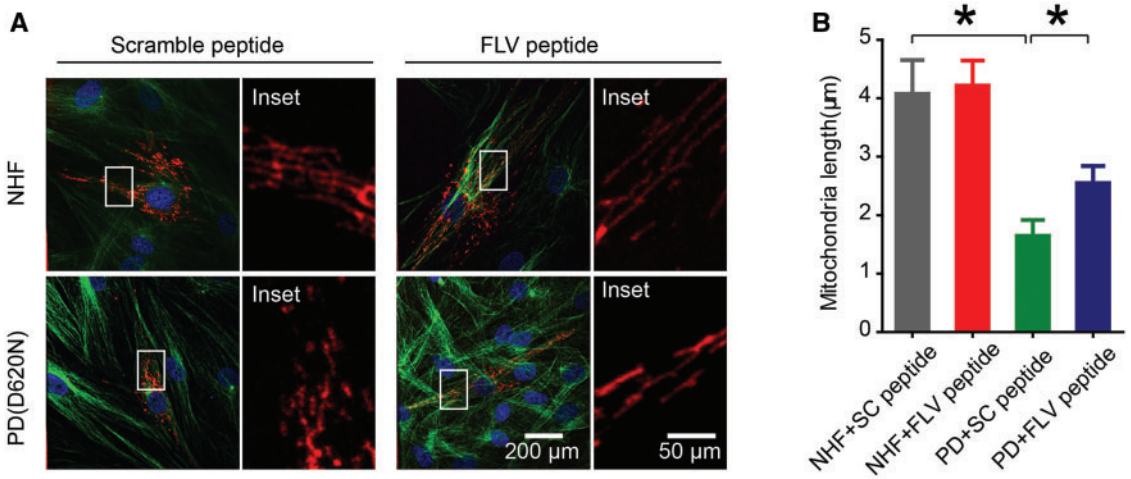

Figure 5. FLV peptide rescued mitochondrial fragmentation in human fibroblasts from PD patient bearing the VPS35 D620N mutation. (**A**) Representative pictures of mitochondria, visualized by mito-DsRed2 fluorescence signal, in normal healthy fibroblasts (NHF) or PD (D620N) fibroblasts treated with scramble peptide or FLV peptide. Boxed area in each picture was enlarged to the right. Red, mito-DsRed2; Green, anti-tubulin; Blue, DAPI. (**B**) Quantification of mitochondrial aspect ratio of NHF and PD (D620N) fibroblasts treated with scramble peptide or FLV peptide. Data are means ± s.e.m of 3 independent experiments. Statistics: one-way analysis of variance (ANOVA) followed by Tukey's multiple comparison test. $^{*}P < 0.05$.

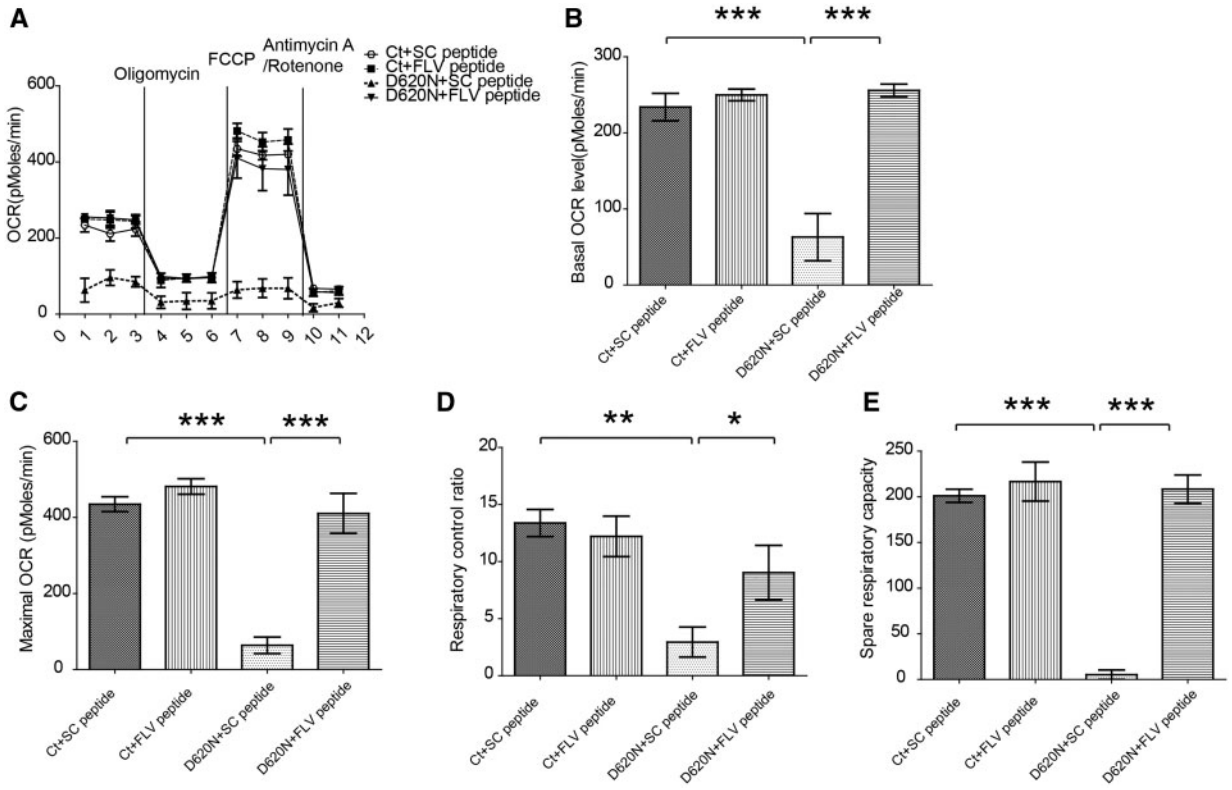

Figure 6. FLV peptide restored mitochondrial respiration in human fibroblasts bearing PD VPS35 D620N mutation. (**A**) Mitochondria respiration activity was measured by Seahorse assay in human fibroblasts treated with scramble peptide or FLV peptide. (**B–E**), Quantification of Basal OCR (B), Maximal OCR (C), Respiratory control ratio (D), and Spare respiratory capacity (E) in these fibroblasts. Data are means ± s.e.m of 3 independent experiments. Statistics: one-way analysis of variance (ANOVA) followed by Tukey's multiple comparison test. $^{*}P < 0.05$, $^{**}P < 0.01$ and $^{***}P < 0.001$.

as demonstrated by co-immunoprecipitation assay. Based on this observation, we designed a decoy peptide with FLV motif and its flanking sequences in DLP1 and treated M17 cells with this peptide. The VPS35-DLP1 interaction was impaired in M17 cells treated with this decoy peptide compared to scramble peptide treatment. These results thus established the FLV motif identified in the C-terminus of DLP1 to be responsible for the recognition and binding of DLP1 by VPS35. The fact that the FLV motif and its flanking sequence are highly conserved between multiple species from zebrafish to human suggests that the involvement of VPS35 and retromer in the regulation of mitochondrial fission through recycling of mitochondrial DLP1 complex is likely a highly conserved step during evolution. Functionally, we found that FLV peptide treatment led to increased mitochondrial DLP1 complex as reflected by both imaging evidence of increased mitochondrial DLP1 puncta and biochemical evidence of increased levels of DLP1 in the 270 Kg super-centrifugation pellet. This observation lends further support to the notion that VPS35-DLP1 interaction is key to the retromer-dependent recycling of mitochondrial DLP1 complex. Consequently, mitochondria became elongated in neurons treated with FLV peptide. More importantly, when we treated M17 cells overexpressing VPS35 D620N mutant or PD D620N fibroblasts, impaired mitochondrial morphology was restored to a level comparable to control cells. Such a rescuing effect on mitochondrial morphology is unlikely due to indirect effect through changes in retromer function since FLV peptide had little effect on retromer regulated recycling of other cargo such as CD36. Considering that FLV peptide did not prevent mitochondrial translocation and oligomerization of DLP1, our data suggest that FLV peptide rescued mitochondrial dynamics deficits by interrupting the VPS35-DLP1 interaction.

The delicate balance of mitochondrial fusion and fission is essential to maintain mitochondrial homeostasis and neuronal function (33). Deficits in mitochondrial fission/fusion genes cause human diseases, especially neurological diseases (34). In fact, a tipped balance towards excessive mitochondrial fission has been implicated in various neurodegenerative diseases including PD (35,36). For example, the first identified PD gene, α-synuclein, was reported to localize to mitochondria and operate downstream of the mitochondrial fusion/fission machinery (13,37). PINK1 and Parkin are involved in the ubiquitination/degradation of fission/fusion proteins and impact mitochondrial dynamics and quality control (38). Another common PD autosomal-dominant gene, LRRK2, regulates mitochondrial translocation of DLP1 through direct interaction (14). Our recent finding of a critical role of VPS35 in the recycling mitochondrial DLP1 complex which was enhanced by D620N mutation lends further support for such a central role of mitochondrial dynamic changes in the pathogenesis of PD (26). Disturbed mitochondrial dynamics could directly cause dopaminergic neuronal death (39). Complex I deficits are consistently reported and likely are causally involved in the process of dopaminergic neuron loss in PD (40) which could also be a result of deficits in the assembly of ETC complexes or supercomplexes caused by mitochondrial dynamic abnormalities (41,42). Recent studies demonstrated that inhibition of DLP1-dependent mitochondrial fission either by genetic or pharmaceutical methods could alleviate dopaminergic neuronal loss in PD models (43),

suggesting mitochondrial dynamic abnormalities as a potential therapeutic target for PD. Given that the VPS35-DLP1 interaction is key in the efficient mitochondrial fission (26), the identification of such a motif critical for VPS35-DLP1 interaction in this study provided opportunities for potential intervention that will be useful for mitochondrial deficits caused by mitochondrial fragmentation due to enhanced VPS35-DLP1 interaction. Indeed, the FLV peptide designed based on the FLV motif of DLP1 to specifically interrupt VPS35-DLP1 binding rescued VPS35 D620N induced mitochondrial fragmentation and respiration in M17 cells expressing VPS35 D620N mutation and in PD fibroblasts with this mutation. This promising therapeutic effect *in vitro* obviously warrants further testing of this FLV peptide *in vivo*. Since paraquat- or hydrogen peroxide-caused the mitochondrial dysfunction also involves increased VPS35-DLP1 interaction (26), this peptide may be of broader use for diseases involving oxidative stress-induced mitochondrial dynamics abnormalities such as idiopathic PD.

In conclusion, we identified a conserved retromer sorting motif in DLP1 which was essential for VPS35 dependent recycling of DLP1 complex on mitochondria in the current study. Based on the motif, we designed a peptide and treated cells with the peptide which could restore impaired mitochondrial dynamics and function in cells with VPS35 mutations. Our studies provided a potential PD therapeutic method targeting to mitochondria dynamic machinery and showed promising treatment effects of the peptide.

Materials and Methods

Cell culture

Human neuroblastoma M17 cells were grown in Opti-MEM medium (Invitrogen), supplemented with 5% (v/v) fetal bovine serum and 1% penicillin–streptomycin (P/S), in 5% CO_2 in a humid incubator at 37 °C. Regular culture medium containing 300 μg/ml geneticin (Invitrogen) was used for stable cell line selection. Primary human fibroblasts from PD patients bearing VPS-35 D620N mutation were characterized previously (23). Primary human fibroblasts from age-matched normal subjects (normal human fibroblasts, NHFs) were obtained from the Coriell Institute for Medical Research. Primary fibroblasts were grown in minimum essential medium (Invitrogen) containing non-essential amino acids and 2 mM glutamine, supplemented with 10% fetal bovine serum, in 5% CO_2 in a humid incubator at 37 °C. Fibroblast cells were transfected with Effectene Transfection Reagent (Qiagen) according to manufacturer's protocol and imaged as we previously reported (44). All cell cultures were tested to be free of mycoplasma contamination.

Plasmids, peptides, and antibodies

Mito-DsRed2 construct (Clontech), the expression plasmids for flag-tagged VPS35 and DLP1 were constructed based on the pCMV-3Flag-1a vector (Agilent) were used. VPS35 and DLP1 mutants were generated by QuikChange Lightning Kit (Agilent). The FLV peptide and scrambled peptide were obtained from GenScript by fusing sorting motif (MHFLVNH) or the scrambled sequence (HLMHFNV) with the transduction domain (YGRKKRRQRRR) of the human immunodeficiency virus TAT protein to enhance peptide delivery. Primary antibodies used included mouse anti-DLP1 (BD Biosciences), mouse anti-Flag (Sigma), rabbit anti-VPS35 (Epitomics), and rabbit anti-CD36 (Santa Cruz).

Mitochondria morphology analysis

M17 cells were seeded into 4-well glass bottom chamber slides (Lab-tek) and transfected with mito-DesRed plasmids for 48 h. Cells then were fixed by 4% paraformaldehyde for 15 min at room temperature and stained by anti-tubulin (Cell Signaling) overnight in a humid chamber at 4 °C. Immunofluorescence images were taken by spinning disk confocal (Perkin Elmer) with HXC PL Fluotar 40X/0.60 air objective. Image analysis was performed by ImageJ and mitochondrial morphology was quantified as previously described (45). Briefly, images were background-corrected, filtered and then threshold to generate binary images. Mitochondrial morphology was indexed as a mitochondrial aspect ratio (ratio between major and minor axes of an ellipse equivalent to the mitochondrion).

Mitochondria cross-link and mitochondrial DLP1 complex assay

M17 cells were seeded into 6-well plates for 24 h. After a wash with PBS, cells were incubated with HBSS containing 0.5 mM dithiobismaleimidoethane (DTME, from freshly prepared stocks in DMSO) for 5 min at 37 °C. The HBSS-DTME was removed and the mitochondrial fraction was isolated. Mitochondria were lysed in buffer containing 60 mM Tris pH 6.8 and 0.2% SDS. Insoluble debris was removed by centrifugation (10 min at 14,000 g) and cleared lysates were layered onto 1 ml of a 300-mM sucrose cushion and subjected to ultracentrifugation (30 min at 270,000 g). These 270,000 g pellets were dissolved in SDS sample buffer containing 5% β-mercaptoethanol to cleave the cross-linker and were analysed by SDS-PAGE.

Western blot and immunoprecipitation

Cells were lysed with RIPA buffer (Abcam), plus 1 mM phenylmethylsulfonyl fluoride (Sigma) and Protease Inhibitor Cocktail (Cell Signaling). Equal amounts of total protein extract (5 or 20 μg) were resolved by sodium dodecyl sulfate polyacrylamide gel electrophoresis and transferred to Immobilon-P (Millipore). Following blocking with 10% nonfat dry milk, primary and secondary antibodies were applied, and the blots were developed with Immobilon western Chemiluminescent HRP Substrate (Millipore). Immunoprecipitation was performed with anti-DLP1/Flag/VPS35 antibodies in RIPA buffer using Dynabeads Protein G-IP Kit (Invitrogen) and analysed by western blot.

Seahorse XF24 mito-stress analysis

The mitochondria respiration assay was carried out as previously reported (26). Briefly, M17 cells were seeded in Seahorse XF-24 (Seahorse Bioscience, Billerica, USA) plates at a density of 100,000 cells per well, which was coated with poly-D lysine (50 μg/ml). For primary fibroblasts, cells were seeded at a density of 50,000 cells per well. Respiration assay was performed in unbuffered DMEM (DMEM base medium supplemented with 25 mM glucose, 1 mM sodium pyruvate, and 1 mM GlutaMAX). The assay protocol consisted of repeated cycles of 3 min mixing, 2 min wait, and 3 min measurement periods. Basal OCR was measured 3 times before drug exposure. Then oligomycin

(1 μM), FCCP (0.5 μM for M17 cells and 2 μM for primary fibroblasts) and Rotenone/antimycin A (0.5 μM) were injected sequentially. After injection of each drug, OCR measurements were made three times. Protein concentrations for each well were measured (BCA method, Pierce) to confirm the comparable cell number in each well.

CD36 receptor recycling assay

Receptor recycling assays were performed as previously described (46) with minor modification. VPS35 M17 cells were seeded in 4-well glass chamber slide at a density of 100,000 cells per well in 5% FBS of Opti-MEM. Culture medium was changed to Opti-MEM with 10% FBS for 2 h at 37 °C, then cells were incubated in Opti-MEM (1% FBS) with antibody against CD36 (Santa Cruz) for 1 h at 37 °C. Cells were acid washed with cold Opti-MEM (pH 2.0) and then were cultured in Opti-MEM with 10% FBS for another 1 h at 37 °C. Cells were incubated in Opti-MEM (1% FBS) with Alexa Fluor 568 conjugated anti-rabbit antibody for 1 h at 37 °C. Cells were again acid washed with cold Opti-MEM at pH 2.0. Cells were fixed with 4% paraformaldehyde for 15 min and permeabilized with 0.5% Triton X-100 for 40 min. Cells were counterstained by DAPI. The recycled fluorescent signal was analysed by ImageJ. Briefly, image background was subtracted by rolling ball radius method and then was thresholded. Averaged thresholded fluorescent signal area was obtained for cells.

Supplementary Material

Supplementary Material is available at *HMG* online.

Conflict of Interest statement. None declared.

Funding

This work is partly supported by the National Institutes of Health [grant numbers NS083385 and NS083498] to X.Z.; by the Chinese Overseas, Hong Kong and Macao Scholars Collaborated Research Fund [grant number 81228007] to X. Z.; by the Dr. Robert M. Kohrman Memorial Fund to X.Z.; by the National Natural Science Foundation of China [grant numbers 81471287, 81071024, 81171202, 81371407, 30872729, 30870879] to J.L.; and by the Shanghai Municipal Education Commission-Gaofeng Clinical Medicine Grant [grant number 20152201] to J.L.

References

1. Rizzo, G., Copetti, M., Arcuti, S., Martino, D., Fontana, A. and Logroscino, G. (2016) Accuracy of clinical diagnosis of Parkinson disease: A systematic review and meta-analysis. *Neurology*, **86**, 566–576.
2. Reichmann, H., Brandt, M.D. and Klingelhoefer, L. (2016) The nonmotor features of Parkinson's disease: pathophysiology and management advances. *Curr. Opin. Neurol.*, **2**, 467–473.
3. Lotharius, J. and Brundin, P. (2002) Pathogenesis of Parkinson's disease: dopamine, vesicles and alpha-synuclein. *Nat. Rev. Neurosci.*, **3**, 932–942.
4. Dauer, W. and Przedborski, S. (2003) Parkinson's disease: mechanisms and models. *Neuron*, **39**, 889–909.
5. Lubbe, S. and Morris, H.R. (2014) Recent advances in Parkinson's disease genetics. *J. Neurol.*, **261**, 259–266.
6. Yan, M.H., Wang, X. and Zhu, X. (2013) Mitochondrial defects and oxidative stress in Alzheimer disease and Parkinson disease. *Free Radic. Biol. Med.*, **62**, 90–101.
7. Bose, A. and Beal, M.F. (2016) Mitochondrial dysfunction in Parkinson's disease. *J. Neurochem.*, **139 Suppl 1**, 216–231.
8. Wang, X., Su, B., Liu, W., He, X., Gao, Y., Castellani, R.J., Perry, G., Smith, M.A. and Zhu, X. (2011) DLP1-dependent mitochondrial fragmentation mediates 1-methyl-4-phenylpyridinium toxicity in neurons: implications for Parkinson's disease. *Aging Cell*, **10**, 807–823.
9. Irrcher, I., Aleyasin, H., Seifert, E.L., Hewitt, S.J., Chhabra, S., Phillips, M., Lutz, A.K., Rousseaux, M.W., Bevilacqua, L., Jahani-Asl, A., *et al.* (2010) Loss of the Parkinson's disease-linked gene DJ-1 perturbs mitochondrial dynamics. *Hum. Mol. Genet.*, **19**, 3734–3746.
10. Wang, X., Petrie, T.G., Liu, Y., Liu, J., Fujioka, H. and Zhu, X. (2012) Parkinson's disease-associated DJ-1 mutations impair mitochondrial dynamics and cause mitochondrial dysfunction. *J. Neurochem.*, **121**, 830–839.
11. Clark, I.E., Dodson, M.W., Jiang, C.G., Cao, J.H., Huh, J.R., Seol, J.H., Yoo, S.J., Hay, B.A. and Guo, M. (2006) Drosophila pink1 is required for mitochondrial function and interacts genetically with parkin. *Nature*, **441**, 1162–1166.
12. Narendra, D., Tanaka, A., Suen, D.F. and Youle, R.J. (2008) Parkin is recruited selectively to impaired mitochondria and promotes their autophagy. *J. Cell Biol.*, **183**, 795–803.
13. Kamp, F., Exner, N., Lutz, A.K., Wender, N., Hegermann, J., Brunner, B., Nuscher, B., Bartels, T., Giese, A., Beyer, K., *et al.* (2010) Inhibition of mitochondrial fusion by alpha-synuclein is rescued by PINK1, Parkin and DJ-1. *Embo J.*, **29**, 3571–3589.
14. Wang, X., Yan, M.H., Fujioka, H., Liu, J., Wilson-Delfosse, A., Chen, S.G., Perry, G., Casadesus, G. and Zhu, X. (2012) LRRK2 regulates mitochondrial dynamics and function through direct interaction with DLP1. *Hum. Mol. Genet.*, **21**, 1931–1944.
15. Vilarino-Guell, C., Wider, C., Ross, O.A., Dachsel, J.C., Kachergus, J.M., Lincoln, S.J., Soto-Ortolaza, A.I., Cobb, S.A., Wilhoite, G.J., Bacon, J.A., *et al.* (2011) VPS35 mutations in Parkinson disease. *Am. J. Hum. Genet.*, **89**, 162–167.
16. Zimprich, A., Benet-Pages, A., Struhal, W., Graf, E., Eck, S.H., Offman, M.N., Haubenberger, D., Spielberger, S., Schulte, E.C., Lichtner, P., *et al.* (2011) A mutation in VPS35, encoding a subunit of the retromer complex, causes late-onset Parkinson disease. *Am. J. Hum. Genet.*, **89**, 168–175.
17. Burd, C. and Cullen, P.J. (2014) Retromer: a master conductor of endosome sorting. *Cold Spring Harb. Perspect. Biol.*, **6**, pii: a016774.
18. Seaman, M.N. (2004) Cargo-selective endosomal sorting for retrieval to the Golgi requires retromer. *J. Cell Biol.*, **165**, 111–122.
19. Bonifacino, J.S. and Rojas, R. (2006) Retrograde transport from endosomes to the trans-Golgi network. *Nat. Rev. Mol. Cell Biol.*, **7**, 568–579.
20. Braschi, E., Goyon, V., Zunino, R., Mohanty, A., Xu, L. and McBride, H.M. (2010) Vps35 mediates vesicle transport between the mitochondria and peroxisomes. *Curr. Biol.*, **20**, 1310–1315.
21. Bonifacino, J.S. and Hurley, J.H. (2008) Retromer. *Curr. Opin. Cell Biol.*, **20**, 427–436.
22. Cullen, P.J. and Korswagen, H.C. (2012) Sorting nexins provide diversity for retromer-dependent trafficking events. *Nat. Cell Biol.*, **14**, 29–37.
23. McGough, I.J., Steinberg, F., Jia, D., Barbuti, P.A., McMillan, K.J., Heesom, K.J., Whone, A.L., Caldwell, M.A., Billadeau, D.D., Rosen, M.K., *et al.* (2014) Retromer binding to FAM21 and the WASH complex is perturbed by the Parkinson

disease-linked VPS35(D620N) mutation. *Curr. Biol.*, **24**, 1670–1676.
24. Tang, F.L., Erion, J.R., Tian, Y., Liu, W., Yin, D.M., Ye, J., Tang, B., Mei, L. and Xiong, W.C. (2015) VPS35 in dopamine neurons is required for endosome-to-Golgi retrieval of Lamp2a, a receptor of chaperone-mediated autophagy that is critical for alpha-synuclein degradation and prevention of pathogenesis of Parkinson's disease. *J. Neurosci.*, **35**, 10613–10628.
25. Munsie, L.N., Milnerwood, A.J., Seibler, P., Beccano-Kelly, D.A., Tatarnikov, I., Khinda, J., Volta, M., Kadgien, C., Cao, L.P., Tapia, L., *et al.* (2015) Retromer-dependent neurotransmitter receptor trafficking to synapses is altered by the Parkinson's disease VPS35 mutation p.D620N. *Hum. Mol. Genet.*, **24**, 1691–1703.
26. Wang, W., Wang, X., Fujioka, H., Hoppel, C., Whone, A.L., Caldwell, M.A., Cullen, P.J., Liu, J. and Zhu, X. (2016) Parkinson's disease-associated mutant VPS35 causes mitochondrial dysfunction by recycling DLP1 complexes. *Nat. Med.*, **22**, 54–63.
27. Tang, F.L., Liu, W., Hu, J.X., Erion, J.R., Ye, J., Mei, L. and Xiong, W.C. (2015) VPS35 deficiency or mutation causes dopaminergic neuronal loss by impairing mitochondrial fusion and function. *Cell Rep.*, **12**, 1631–1643.
28. Yun, J., Puri, R., Yang, H., Lizzio, M.A., Wu, C., Sheng, Z.H. and Guo, M. (2014) MUL1 acts in parallel to the PINK1/parkin pathway in regulating mitofusin and compensates for loss of PINK1/parkin. *eLife*, **3**, e01958.
29. Seaman, M.N. (2007) Identification of a novel conserved sorting motif required for retromer-mediated endosome-to-TGN retrieval. *J. Cell Sci.*, **120**, 2378–2389.
30. Merrill, R.A., Dagda, R.K., Dickey, A.S., Cribbs, J.T., Green, S.H., Usachev, Y.M. and Strack, S. (2011) Mechanism of neuroprotective mitochondrial remodeling by PKA/AKAP1. *PLoS Biol.*, **9**, e1000612.
31. Fjorback, A.W., Seaman, M., Gustafsen, C., Mehmedbasic, A., Gokool, S., Wu, C., Militz, D., Schmidt, V., Madsen, P., Nyengaard, J.R., *et al.* (2012) Retromer binds the FANSHY sorting motif in SorLA to regulate amyloid precursor protein sorting and processing. *J. Neurosci.*, **32**, 1467–1480.
32. Tabuchi, M., Yanatori, I., Kawai, Y. and Kishi, F. (2010) Retromer-mediated direct sorting is required for proper endosomal recycling of the mammalian iron transporter DMT1. *J. Cell Sci.*, **123**, 756–766.
33. Okamoto, K. and Shaw, J.M. (2005) Mitochondrial morphology and dynamics in yeast and multicellular eukaryotes. *Ann. Rev. Genet.*, **39**, 503–536.
34. Chan, D.C. (2006) Mitochondria: dynamic organelles in disease, aging, and development. *Cell*, **125**, 1241–1252.
35. Su, B., Wang, X., Zheng, L., Perry, G., Smith, M.A. and Zhu, X. (2010) Abnormal mitochondrial dynamics and neurodegenerative diseases. *Biochim. Biophys. Acta*, **1802**, 135–142.
36. Chen, H. and Chan, D.C. (2009) Mitochondrial dynamics–fusion, fission, movement, and mitophagy–in neurodegenerative diseases. *Hum. Mol. Genet.*, **18**, R169–R176.
37. Guardia-Laguarta, C., Area-Gomez, E., Rub, C., Liu, Y., Magrane, J., Becker, D., Voos, W., Schon, E.A. and Przedborski, S. (2014) alpha-Synuclein is localized to mitochondria-associated ER membranes. *J. Neurosci.*, **34**, 249–259.
38. Chu, C.T. (2010) Tickled PINK1: mitochondrial homeostasis and autophagy in recessive Parkinsonism. *Biochim. Biophys. Acta*, **1802**, 20–28.
39. Pham, A.H., Meng, S., Chu, Q.N. and Chan, D.C. (2012) Loss of Mfn2 results in progressive, retrograde degeneration of dopaminergic neurons in the nigrostriatal circuit. *Hum. Mol. Genet.*, **21**, 4817–4826.
40. Abou-Sleiman, P.M., Muqit, M.M. and Wood, N.W. (2006) Expanding insights of mitochondrial dysfunction in Parkinson's disease. *Nat. Rev. Neurosci.*, **7**, 207–219.
41. Liu, W., Acin-Perez, R., Geghman, K.D., Manfredi, G., Lu, B. and Li, C. (2011) Pink1 regulates the oxidative phosphorylation machinery via mitochondrial fission. *Proc. Natl. Acad. Sci. U. S. A*, **108**, 12920–12924.
42. Cogliati, S., Frezza, C., Soriano, M.E., Varanita, T., Quintana-Cabrera, R., Corrado, M., Cipolat, S., Costa, V., Casarin, A., Gomes, L.C., *et al.* (2013) Mitochondrial cristae shape determines respiratory chain supercomplexes assembly and respiratory efficiency. *Cell*, **155**, 160–171.
43. Rappold, P.M., Cui, M., Grima, J.C., Fan, R.Z., de Mesy-Bentley, K.L., Chen, L., Zhuang, X., Bowers, W.J. and Tieu, K. (2014) Drp1 inhibition attenuates neurotoxicity and dopamine release deficits in vivo. *Nat. Commun.*, **5**, 5244.
44. Wang, X., Su, B., Fujioka, H. and Zhu, X. (2008) Dynamin-like protein 1 reduction underlies mitochondrial morphology and distribution abnormalities in fibroblasts from sporadic Alzheimer's disease patients. *Am. J. Pathol.*, **173**, 470–482.
45. Wang, X., Su, B., Lee, H.G., Li, X., Perry, G., Smith, M.A. and Zhu, X. (2009) Impaired balance of mitochondrial fission and fusion in Alzheimer's disease. *J. Neurosci.*, **29**, 9090–9103.
46. Lucin, K.M., O'Brien, C.E., Bieri, G., Czirr, E., Mosher, K.I., Abbey, R.J., Mastroeni, D.F., Rogers, J., Spencer, B., Masliah, E., *et al.* (2013) Microglial beclin 1 regulates retromer trafficking and phagocytosis and is impaired in Alzheimer's disease. *Neuron*, **79**, 873–886.